JACS
JOURNAL OF THE AMERICAN CHEMICAL SOCIETY

ARTICLE

pubs.acs.org/JACS

Kubas-Type Hydrogen Storage in V(III) Polymers Using Tri- and Tetradentate Bridging Ligands

Tuan K. A. Hoang,[†] Ahmad Hamaed,[†] Golam Moula,[†] Ricardo Aroca,[†] Michel Trudeau,[‡] and David M. Antonelli*[,†,§]

[†]Department of Chemistry and Biochemistry, University of Windsor, 401 Sunset Avenue, Windsor, Ontario N9B 3P4, Canada

[‡]Emerging Technologies, Hydro-Québec Institute, 1800 Boul. Lionel-Boulet, Varennes, Quebec J3X 1S1, Canada

[§]Sustainable Environment Research Center, University of Glamorgan, Pontypridd CF37-1DL, United Kingdom

Supporting Information

ABSTRACT: Oxalic acid, oxamide, glycolic acid, and glycolamide were employed as 2-carbon linkers to synthesize a series of one-dimensional V(III) polymers from trismesityl vanadium(III)·THF containing a high concentration of low-valent metal sites that can be exploited for Kubas binding in hydrogen storage. Synthesized materials were characterized by powder X-ray diffraction (PXRD), nitrogen adsorption (BET), X-ray photoelectron spectroscopy (XPS), infrared spectroscopy (IR), Raman spectroscopy, thermogravimetric analysis, and elemental analysis. Because each of these organic linkers possesses a different number of protons and coordinating atoms, the products in each case were expected to have different stoichiometries with respect to the number of mesityl groups eliminated and also a different geometry about the V(III) centers. For example, the oxalate and glycolate polymers contained residual mesityl groups; however, these could be exchanged with hydride via hydrogenolysis. The highest adsorption capacity was recorded on the product of trismesityl vanadium(III)·THF with oxamide (3.49 wt % at 77 K and 85 bar). As suggested by the high enthalpy of adsorption (17.9 kJ/mol H_2), a substantial degree of performance of the vanadium metal centers was retained at room temperature (25%), corresponding to a gravimetric adsorption of 0.87 wt % at 85 bar, close to the performance of MOF-177 at this temperature and pressure. This is remarkable given the BET surface area of this material is only 9 m^2/g. A calculation on the basis of thermogravimetric results provides 0.88 hydrogen molecule per vanadium center under these conditions. Raman studies with H_2 and D_2 showed the first unequivocal evidence for Kubas binding on a framework metal in an extended solid, and IR studies demonstrated H(D) exchange of the vanadium hydride with coordinated D_2. These spectroscopic observations are sufficient to assign the rising trends in isosteric heats of hydrogen adsorption observed previously by our group in several classes of materials containing low-valent transition metals to the Kubas interaction.

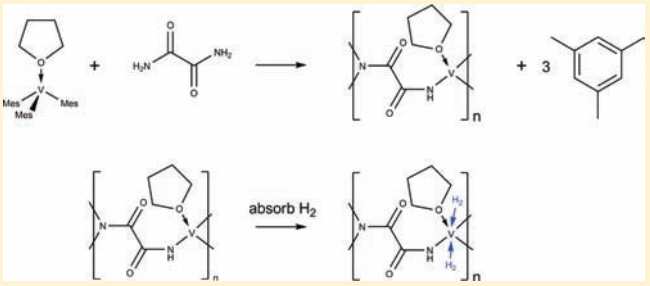

INTRODUCTION

Hydrogen is one of the best candidates for an alternative energy carrier and in its pure form can be stored in compressed gas cylinders at pressures as high as 700 bar. Since these pressures are considered unsafe and the ranges of vehicles using such tanks are still not optimal, new methods of storing hydrogen are currently being investigated.[1] Extensive research has been carried out using a variety of systems as chemical carriers based around physisorption[2] and metal hydrides;[3] however, these approaches have so far fallen short of the U.S. Department of Energy (DOE) 2015 system target[4] of 5.5 wt % and 40 kg/m^2 H_2 at 298 K. Some chemical hydrides, which generally possess high adsorption enthalpies in the 70 kJ/mol range, contain enough hydrogen to satisfy the DOE 2015 target;[5] however, the kinetics of charging and discharging hydrogen and the heat management issues prevent them from practical usage.[6] Catalyzed hydrogen spillover on high surface area substrates,[7] is another promising method employing dissociative hydrogen adsorption; however, it too has yet to meet the stringent DOE goals. Physisorption materials, such as carbon[8] and metal−organic frameworks (MOFs),[9] possess much lower binding enthalpies (5−13 kJ/mol) and demonstrate excellent hydrogen uptake with no kinetic barrier and little heat management issues at 77 K and moderate pressure. For example, the total hydrogen uptake of MOF-177 and NOTT-122 surpasses the DOE 2015 system target under these conditions;[10] however the cost of cooling still makes this technology prohibitive. To improve performance at higher temperatures, some MOF materials have been synthesized in hopes to exploit the role of open metal sites[11] or the Kubas interaction,[12] a type of hydrogen binding to transition metals with enthalpies in the 20−50 kJ/mol range.[13−15] While there has yet to be conclusive spectroscopic evidence of the Kubas interaction in MOFs, it has been observed by vibrational spectroscopy in Cu-ZSM-5.[16]

Received: November 23, 2010
Published: March 10, 2011

Extensive studies of metal binding sites have also been carried out by our group on Ti, V, Cr supported silica systems using different oxidation states, ligand types, preparation methods, and doping levels.[17,18] In these studies, Ti(III), V(III), Cr(II), and Cr(III) were identified as the best metal hosts for what was believed to be Kubas interaction with hydrogen at room temperature and moderate pressure on the basis of rising enthalpies with surface covereage.[19] Subsequent computational studies have supported this assignment;[20] however, no spectroscopic evidence has yet been obtained due to the small amounts of hydrogen absorbed by the ca. 5% metal in these systems. To maximize the number of potential Kubas sites per unit volume, cyclopentadienyl chromium hydrazide gels[21] and vanadium hydrazide gels[22] were synthesized by the reaction of low valent organometallic precursors with anhydrous hydrazine. Hydrazine was used as a linker because of its low molecular weight and ability to bridge two metal centers, providing a diffusion pathway for hydrogen without creating excess void space, while also maintaining the low ligation number of the metal coordination sphere. These X-ray amorphous materials possess linear isotherms at both 77 and 298 K that do not saturate at 80 bar, ideal adsorption enthalpies in the 20−40 kJ/mol range, and maintain up to 49% of their performance at 298 K as compared to 77 K. The volumetric adsorption of the vanadium material at 77 K and 80 bar (60 kg/m^3) surpasses all MOFs as well as the 2010 DOE target. At room temperature, this material demonstrates a volumetric adsorption of 23.2 kg/m^3 H_2, approaching the 2010 DOE target. While transition metal hydrazides show enormous promise, hydrazine has many safety issues and can also bind in multiple coordination modes, leading to amorphous systems that are difficult to characterize. Because of this, we are continuing to explore other low-molecular weight ligands that support low-coordinate metal sites useful for Kubas binding. In this work, trismesitylvanadium(III)·THF was treated with various commercially available multiproton, multidentate chelating ligands capable of bridging two metal centers in a controlled stoichiometric fashion. The one-to-one metal-to-ligand stoichiometry used in this study should also favor a 1-D system with much more flexibility around the tetrahedral metal center than more rigid 3-D systems such as zeolites,[23] which do not possess a high number of active and strong adsorption centers per unit volume, to optimize the orbital geometries for H_2 coordination.

EXPERIMENTAL SECTION

All chemicals, unless otherwise stated, were obtained from Aldrich. H_2 grade 6.0, N_2, Ar, and He were obtained from Praxair Canada. All solvents were dried by distillation in argon atmosphere, using sodium/benzophenone to remove moisture and oxygen. Distilled solvent was transferred to a Schlenk flask using a canula. Dry argon gas was bubbled through the flask for 30 min, followed by degassing before transferring into a drybox.

Preparation of V(Mes)$_3$·THF. 33.33 mL of dry tetrahydrofuran (THF) was added to 50 mL of mesityl magnesiumbromide 1 M (MesMgBr) solution in THF, followed by the portion-by-portion addition of 6.22 g of VCl_3·3THF 97%. The resulting solution was stirred vigorously at room temperature for 2 h, and a clear blue solution was obtained. 21.66 mL of dioxane was then added to the solution with stirring. After 2 more hours, stirring was ceased, and the solution was left to settle before filtration. The filtrate was collected and concentrated in a vacuum until crystals formed. 16.67 mL of diethylether was then added, and the remaining product precipitated out. The solid product was then collected by filtration and washed several times with a solution of THF and ether (THF:ether = 1:3 by volume) before drying in a vacuum.[24]

Preparation of V-Oxamide100 and V-Oxamide150. V-Oxamide100 was synthesized as follows: V(Mes)$_3$·THF (3 g, 6.24 mmol) was dissolved in 75 mL of dry toluene at room temperature in an Erlenmeyer flask. 0.5608 g (6.24 mmol) of oxamide was then added with vigorous stirring. The solution was capped and stirring was continued for 12 h. The solution was then heated to 100 °C for 3 h with stirring. After this, the system was filtered, and a black solid was obtained. The filtrate was colorless, indicating complete reaction of the V precursor. This solid was transferred to an air-free tube and was then dried under a vacuum (10^{-2} mmHg) for 12 h, followed by heating at 60 °C under a vacuum (10^{-2} mmHg) for a period of 6 h and another 6 h at 100 °C under a vacuum (10^{-2} mmHg). V-Oxamide150 was obtained by continuing to heat V-Oxamide100 at 150 °C for 6 h in a vacuum (10^{-2} mmHg).

Preparation of V-Oxalate150, V-Glycolate150, and V-Glycolamide150. V-Oxalate150 was synthesized by the same method as V-Oxamide150, using 0.5618 g (6.24 mmol) of oxalic acid instead of oxamide. V-Glycolate150 and V-Glycolamide150 were also synthesized in this same way, using glycolic acid (0.4973 g; 6.24 mmol) and glycolamide (0.4780 g; 6.24 mmol), respectively. The filtrate was colorless in each case, indicating complete reaction of the V precursor.

Preparation of H_2-V-Oxalate and H_2-V-Glycolate. V-Oxalate150 and V-Glycolate150 were treated with hydrogen at 150 °C and 85 bar for 3 h, and the resulting materials were then collected and stored under Ar.

Analysis. Powder X-ray diffraction (PXRD) was performed on a Siemens diffractometer D-500 with Cu Kα radiation (40 KV, 40 mA) source. The step size was 0.02°, and the counting time was 0.3 s for each step. Diffraction patterns were recorded in the 2θ range of 2.3−52°. Samples for PXRD analysis were put in a sealed capillary glass tube to protect the sample from air and moisture during experiment.

Nitrogen adsorption and desorption data were collected on a Micromeritics ASAP 2010. All XPS studies were conducted using a Physical Electronics PHI-5500 spectrometer using charge neutralization, and emissions were referenced to the carbon C−(C, H) peak at 284.8 eV. Elemental analysis was performed by Galbraith Laboratories, Knoxville, TN. Thermogravimetric analysis was conducted on a Mettler Toledo TGA SDTA 851e, using helium (99.99%) as purging gas with the rate of 30 mL/min. Samples were held at 25 °C for 20 min before being heated to 550 °C at a rate of 5 °C/min.

FT-IR was conducted on all synthesized materials using a Bruker Vector 22 instrument. In a typical experiment, 2 mg of sample was mixed with 500 mg of dry KBr, and a compressed disk was made in an inert atmosphere. The discs were then transferred outside, and the measurements were conducted immediately. Because this technique was primarily used to identify the hydrocarbon in the sample, which would not oxidize on exposure to air, rigorously air-free conditions were not employed.

Hydrogen−Deuterium Exchange Experiment. 100 mg of V-Oxamide150 was placed in a Schlenk tube connected to a bubbler and a deuterium cylinder. A deuterium stream was passed over the sample for 7 days at a rate of 1 L per hour. After this, the deuterium-treated sample was left under a vacuum for 6 h. The original and deuterium treated materials were then studied by infrared spectroscopy using a Bruker Tensor 27 instrument. Three milligrams of material was mixed with 500 mg of KBr, and a compressed disk was made in inert atmosphere. The discs were transferred outside, and the measurements were conducted immediately.

Raman Experimental Details. Samples were loaded in NMR tubes fitted with Young's valves, and spectra were recorded under 1 atm of H_2, D_2, or Ar. For the samples recorded after vacuum, the samples were left for 1 h under H_2 or D_2 and then placed under vacuum for 10 min before backfilling with Ar. All micro-Raman scattering experiments were

Scheme 1. Proposed Reaction between V(Mes)$_3$·THF and Various Ligands: (a) Oxamide, (b) Oxalic Acid, (c) Glycolic Acid, and (d) Glycolamide

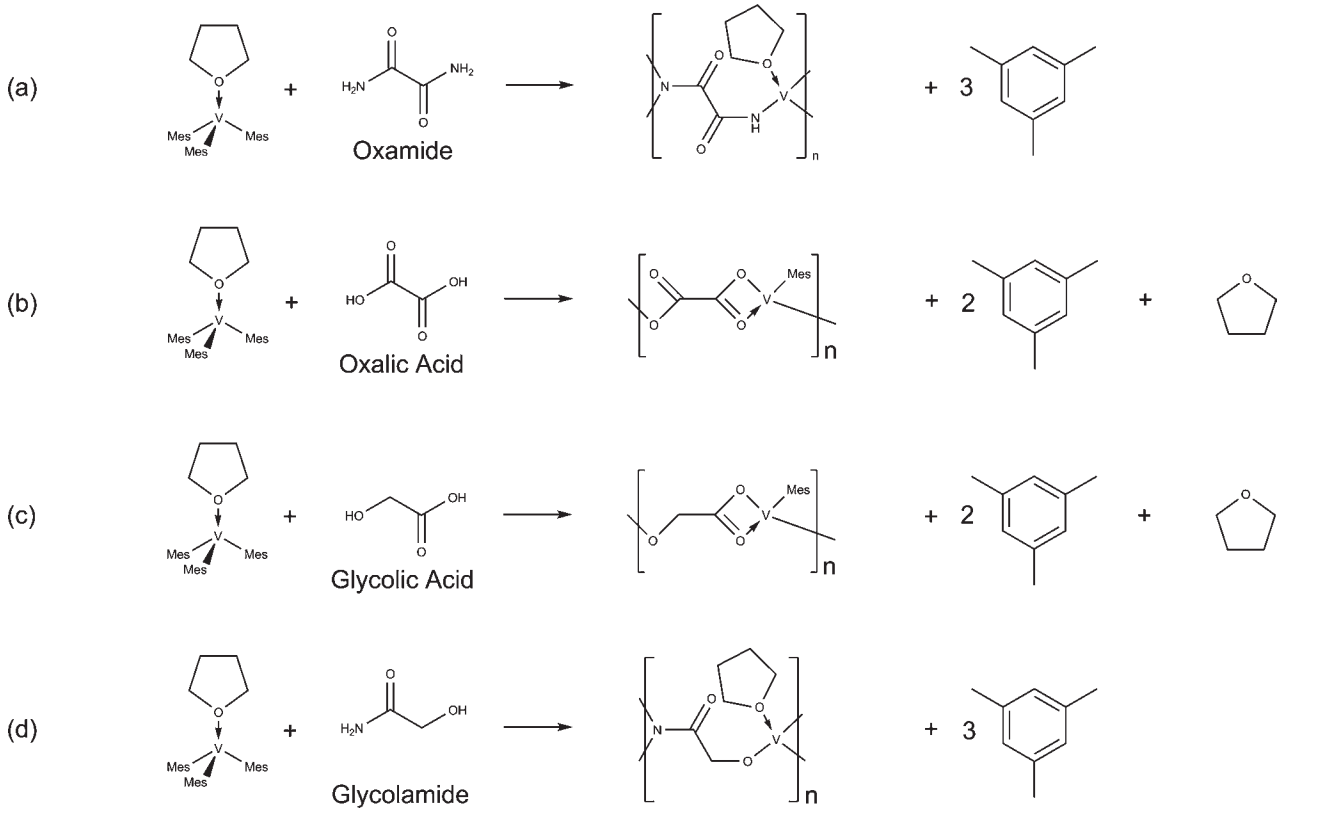

conducted using a Renishaw InVia system, with laser excitation at 514.5 nm, and powers of 10−20 μW at the sample. Each scan was duplicated to ensure that any features observed were reproducible. All measurements were made in a backscattering geometry, using a 20× microscope objective with a numerical aperture value of 0.40, providing scattering areas of ~20 μm^2. Single-point spectra were recorded with 4 cm^{-1} resolution and 50 s accumulation times. Data acquisition and analysis were carried out using the WIRE software for windows and Galactic Industries GRAMS C software.

Hydrogen Adsorption Measurements. Hydrogen adsorption isotherms were obtained by using an Advanced Materials PCI and the same method described in our previous publications on metal hydrazides.[21,22] Adsorption enthalpies were calculated from adsorption isotherms at 77 and 87 K, using a method described elsewhere.[25] True volumetric adsorption of all materials were calculated on the basis of gravimetric adsorption and skeletal densities of materials, while absolute volumetric adsorption was calculated on the basis of gravimetric adsorption using bulk densities.[25,26]

RESULTS AND DISCUSSION

In this work, tris(mesityl) vanadium(III)·THF was treated with one molar equivalent of either oxamide, oxalic acid, glycolic acid, and glycolamide to create polymers with V−O and V−N linkages through protonolysis of the mesityl groups. The samples were then dried at either 100 or 150 °C (to create, for example, V-Oxamide100 or V-oxamide150, respectively), and their hydrogen storage properties were tested. Because the materials dried at 150 °C possessed superior hydrogen storage performance, the majority of this Article focuses on these samples. The proposed reaction of V(Mes)$_3$·THF with the various ligands is shown in Scheme 1.

The four protons present in oxamide are enough to eliminate three mesityl groups with one proton remaining, putatively resulting in a tetrahedral V(III) center bound to 2 O and 2 N atoms from oxamide, capable of binding 3 H_2 according to the 18-electron rule.[27] Because the expected weight of the V-oxamide monomer is 136 g/mol, this corresponds to 4.41 wt % H_2, close to the 2010 DOE goal. Oxalic acid has only two protons per ligand so one remaining mesityl is expected in V-oxalate, resulting in a five-coordinate environment with the 4 oxalate oxygens, while in the glycolate material there are only two available protons and three ligating atoms, so retention of one aryl group to create a 4-coordinate center V(III) is expected. In the glycolamide material, there are three protons available and three ligating atoms per ligand; however, elimination of all three mesityls would result in a three-coordinate V center, which is not likely. Therefore, it is possible that there is a remaining aryl functionality on the V-center with a proton still remaining on the ligand, or conversely that all mesityls have been eliminated and the extra coordination site is taken up by THF, which could be clarified by XPS and IR spectroscopy.

The PXRD pattern (Figure S1a−f; Supporting Information) of V-Oxamide150 showed a wide reflection at $2\theta < 5°$, suggesting possible mesoscopic periodicity with no long-range order in the material. Similar XRD patterns were obtained with vanadium hydrazide gels, which were synthesized by employing the same V(Mes)$_3$·THF precursor, but with anhydrous hydrazine as linking agent.[22] The materials synthesized from oxalic acid,

dx.doi.org/10.1021/ja110243r |J. Am. Chem. Soc. 2011, 133, 4955–4964

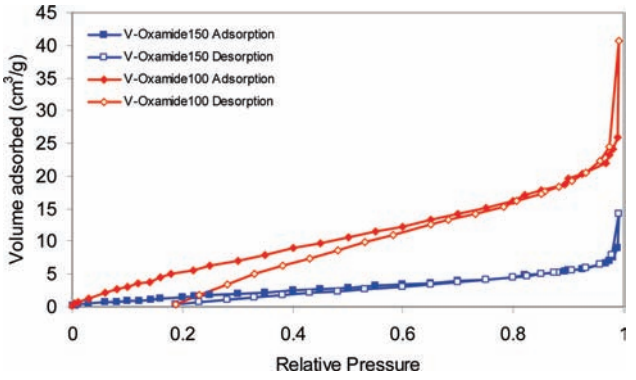

Figure 1. Nitrogen adsorption−desorption isotherms of V-Oxamide100, V-Oxamide150. Samples were measured on an ASAP-2010 instrument at 77 K.

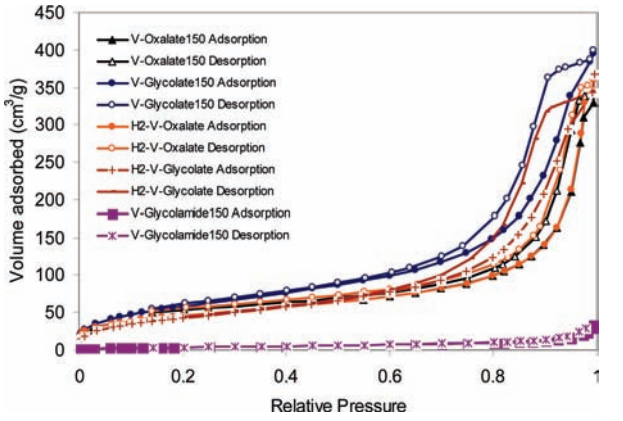

Figure 2. Nitrogen adsorption−desorption isotherms of V-Oxalate150, V-Glycolate150, H_2-V-Oxalate150, H_2-V-Glycolate150, and V-Glycolamide150.

glycolic acid, or glycolamide do not possess any distinct XRD feature and appear to be completely amorphous. Nitrogen adsorption and desorption isotherms for these materials displayed Brunauer−Emmett−Teller (BET) surface areas in the range of 9−220 m^2/g (Figures 1 and 2). The isotherms were all type II, representing nonporous materials with most of the surface area arising from textural porosity.[28] Similar isotherms and surface areas were observed for V- and cyclopentadienyl Cr-hydrazide gels studied previously by our group.[21,22] The isotherms for the V-Oxamide materials show anomalies in the desorption branch passing under the adsorption branch, which can be attributed to the very low surface areas of these materials (9 and 28 m^2/g) approaching the detection limit of the instrument on the sample sizes used in the measurement.

The C, H, N, and V elemental analysis data of these materials are shown in Table S1, and the expected molecular formulas and compositions of the stoichiometric products are shown in Table S2 (Supporting Information). The high carbon values for the oxamide and glycolamide samples indicate that the reaction did not go to completion, either due to retention of THF or because of incomplete protolysis of the mesityl groups. In contrast, the carbon values for the oxalic acid and glycolic acid samples were lower than expected, perhaps due to incomplete combustion of the material during the elemental analysis process leading to carbide formation. The V values are systematically low, potentially due to incomplete reaction stoichiometries or error in the elemental analysis process due to incomplete digestion of the V species in HF, so these values may not reflect the true V content in the materials. Repeat analysis yielded similar results, so this may reflect the limitations of this technique on these materials.

Infrared spectroscopy (IR) was also used to characterize the materials. All samples show strong stretches for metal-coordinated carbonyl groups at ca. 1600 cm^{-1}. The elimination of hydrocarbon was supported by the decrease in intensity of the C−H stretches at 2850−2950 cm^{-1} in the spectrum of the products as compared to $V(Mes)_3 \cdot THF$ (Figure S2; Supporting Information). Because V-glycolate150 and V-glycolamide150 contain methylene protons in the α-carbon to the carbonyl, it is not possible to distinguish the C−H stretches arising from these functionalities from those of residual mesitylene. The C−C aromatic stretches expected at 1500 cm^{-1} in all materials are obscured by other bands and are therefore not useful in this study. The IR spectrum of the V-Oxamide150 shows an unusual feature at 2200 cm^{-1} that can be assigned to a V−H.[29] The presence of this species must arise from migration of the additional hydrogen atom from the organic ligand to the V center through an α-hydrogen migration.[30] Because only three of the four oxamide protons are used in eliminating the aryl groups, the remaining proton, not present in the other three ligands, is free to migrate to the V(III) center.

XPS studies of the synthetic materials were conducted, and the results are shown in Figures S3−S6 (Supporting Information). In general, these spectra support the formulations suggested by the IR spectra, but expand on our knowledge of the oxidation states and binding modes present in each material. Multiple oxidation states of vanadium were detected in the vanadium 2p 1/2, 3/2 regions of all samples (Figure S3; Supporting Information). For V-Oxamide150, a small amount of a V(I) species is detected at 513.8 and 519.7 eV, assigned by comparison with literature values.[31] Emissions at 515.1 and 521.9 eV can be assigned to V(III).[32] V(IV) species are also present at 516.2 and 523.4 eV.[33] V(V) is detected with emissions at 517.6 and 524.9 eV.[34] Similar disproportionation was observed for vanadium hydrazides studied by our group and is common in the chemistry of lower oxidation sates of this element. Four oxidation states of vanadium were also detected in V-Oxalate150 and V-Glycolate150, but the emissions are slightly shifted to higher binding energies with ~0.3 eV difference. The V-glycolamide150 material also has multiple oxidation states, but there appear to be no V(I) species present. The reason for this is not understood but may be related to the relative disproportionation pathways open to the metals in the different ligand environments.

The O 1s region of the XPS spectra of all materials is shown in Figure S4. The emission at 530.4 eV, which is very strong in the case of V-Oxamide150 and moderately strong in the case of V-Glycolamide150, can be attributed to coordinated THF on the basis of our previous work on vanadium hydrazides, which show a substantial amount of THF retention.[22] This is consistent with the EA of these materials, which exhibits a higher amount of carbon than expected. The fact that the THF is not observed in the glycolate or oxalate samples is consistent with the presence of the one remaining sterically demanding mesityl group expected by proton stoichiometry. The emission at 532 eV can be attributed to V-bound oxygen in the amide carbonyl or carboxylate group in all four species on the basis of previous XPS spectra of metal coordinated carboxylate species,[35,36] while the small

emission at 533.8 eV corresponds to an oxygen with two single bonds in either C−O−V or C−O−H species.[37] The latter would be expected in the oxamide and glycolamide materials due to tautomerization of the amide functionality. The N 1S XPS spectrum of V-Oxamide150 shows a large peak, which can be simulated as three emissions at 396.8, 398.8, and 400.3 eV (Figure S5; Supporting Information). As compared to the values reported for monomeric compounds, the emission at 400.3 eV could be attributed to a bound nitrogen from a $-(C{=}O)-NH_2$ species.[38] The emission at 398.8 eV can be assigned to the nitrogen in $-(C{=}O)-NH-$ species on the basis of previous XPS on metal coordinated amides.[35,39] The small emission at 396.7 eV can be attributed to a free amino N bound directly to two vanadium centers,[40] possibly formed through a small amount of reductive C−N cleavage due to decomposition. The high intensity of the central emission being assigned to a proton-free N species is consistent with three of the four oxamide protons being used to eliminate the aryl group. The XPS of the N 1s region of V-Glycolamide150 can be simulated as two peaks at 400.2 and 398.8 eV and can thus be assigned to analogous $-(C{=}O)-NH_2$ and $-(C{=}O)-NH-$ species by comparison to the oxamide species. The presence of N−H is consistent with incomplete elimination of the aryl group. No emission is detected at 396.8 eV, indicating that there are no free amino groups in the materials. This can be further confirmed by IR, as there are N−H stretches present from 3400−3500 cm^{-1} in V-Oxamide150 but not in the IR of the other materials. XPS of all samples in the valence region were also obtained (Figure S6; Supporting Information). All materials with the exception of V-Oxamide 150 display a high density of states at the Fermi level consistent with metallic behavior in these samples. This was confirmed by the fact that charge neutralization was only required on the oxamide sample.

To gain further insight into the composition of these materials, we performed thermogravimetric analysis (TGA), which is often used as a compliment to elemental analysis. The TGA curves for all four samples are shown in the Supporting Information (Figure S7) and show a steady drop in mass with heating at a rate of 5 °C/min from 200 to 350 °C, followed by a more gradual decrease to 550 °C. For V-oxamide150, 45.09% mass was remaining at the end of the experiment. Assuming complete conversion to V_2O_5, the %V in the original sample would be 25.26%. If the molecular formula of this material was $C_2HN_2O_2V$, then 37.46% of the sample would be V, with 66.87% mass remaining after stoichiometric conversion to V_2O_5. If 1 THF per V center is included, as suggested by the IR and XPS, then the material would have a formula of $C_6H_9N_2O_3V$, with 24.48% V and 43.7% mass remaining after conversion to V_2O_5. The TGA data are thus more consistent with the later formulation of this material as a THF adduct as given in Table S2. Likewise, V-Glycolamide150 can be formulated more accurately as a THF adduct on the basis of 50.95% mass remaining after combustion, while the remaining glycolic and oxalic acid materials appear to be correctly formulated as described in Scheme 1, with 49.13% and 42.01% mass remaining, respectively, after combustion in the TGA experiment. The %V as derived from TGA is shown for all materials in Table S1 and in all cases more closely matches the expected values listed in Table S2 than do the EA results.

Figure 3 shows the excess hydrogen adsorption and desorption isotherms at 77 K and excess hydrogen adsorption at 298 K of the V-Oxamide100 and V-Oxamide150 materials. The hydrogen storage results for this and other samples are summarized in Table 1. At 77 K, there is an initial sharp rise to ~0.5 wt % at the beginning of adsorption process, followed by linear region up to 85 bar. The cyclopentadienyl chromium hydrazide materials synthesized by our group possess similar adsorption isotherms with a sharp rise at low pressure.[21] This can be attributed to a small amount of physisorption arising from the relatively low surface area of the material and the adsorption of hydrogen molecules on the outermost adsorption centers, which are coordinatively unsaturated and exposed. At 85 bar, V-Oxamide100 adsorbs 2.25 wt % hydrogen at 77 K and 0.51 wt % at 298 K (Table 1). Increasing the activation temperature to 150 °C affords a material with 3.49 wt % adsorption at 77 K and 85 bar. From 0 to 30 bar, this material adsorbs up to 0.55 wt % at 298 K. After that, the isotherm is linear up to 85 bar, and an adsorption capacity of 0.87 wt % is achieved. These results correspond to a true volumetric density of 51 kg/m^3 at 77 K and 13 kg/m^3 at room temperature. The true volumetric density was quoted previously by our group for vanadium hydrazide gels and is defined as the product of the skeletal density and the excess storage.[22] While it is not typical in the physorption of carbons and MOFs to use the skeletal densities in calculating the volumetric density, this is because of the large amount of void space in these materials and the correspondingly large discrepancy between the bulk density and skeletal density. In our polymeric materials, the void space has been minimized to optimize the amount of adsorption arising from Kubas sites, so there is only a small difference between skeletal density and bulk density. The absolute volumetric adsorption of V-Oxamide150 material was obtained by using a preweighed portion of material, which was compressed at 500 psi pressure to remove void spaces between particles. The compressed material possesses a bulk density of 0.9739 g/cm^3. At 85 bar, it adsorbs 2.25 wt % of hydrogen at 77 K and 0.99 wt % at 298 K. This corresponds to an absolute volumetric adsorption of 21.91 and 9.6 kg/m^3, respectively, at 77 and 298 K. This compares to an absolute volumetric adsorption of 30 kg/m^3 for MOF 177 and a volumetric storage of MOF-177, including the compressed gas, of 50.3 kg/m^3 at 77 K and 8 kg/m^3 at 298 K.[26] Because V-Oxamide150 adsorbs hydrogen in a linear fashion without saturation at 80 bar and 298 K, this indicates that higher adsorption results could be expected at higher pressures.

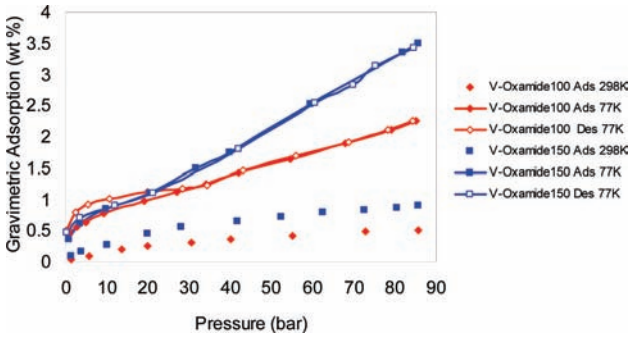

Figure 3. Excess hydrogen adsorption isotherms at 77 K, 298 K of V-Oxamide100, V-Oxamide150. Desorption at 298 K is left out for clarity.

The excess storage isotherms of V-Oxalate150, V-Glycolate150, and V-Glycolamide150 are shown in Figures 4, 5, and 6, respectively. At 77 K, a sharp initial rise up to 0.65 wt % from 1 to 10 bar is observed in V-Oxalate150. This is attributed to

Table 1. Summary of Excess Storage Data on Various Vanadium Materials and Carbon AX-21[a]

material	BET surface area (m^2/g)	skeletal density (g/cm^3)	gravimetric adsorption (wt %)	volumetric adsorption (kg/m^3)	retention (%)
V-Oxamide100	28	1.2308	2.25 (at 77 K)	28 (at 77 K)	23
			0.51 (at 298 K)	6.2 (at 298 K)	
V-Oxamide150	9	1.4636	3.49 (at 77 K)	51 (at 77 K)	25
			0.87 (at 298 K)	13 (at 298 K)	
V-Oxalate150	168	1.6452	1.10 (at 77 K)	18 (at 77 K)	21
			0.23 (at 298 K)	3.8 (at 298 K)	
H_2-V-Oxalate	169	1.4581	1.40 (at 77 K)	20 (at 77 K)	32
			0.44 (at 298 K)	6.4 (at 298 K)	
V-Glycolate150	220	1.4407	1.60 (at 77 K)	23 (at 77 K)	17
			0.28 (at 298 K)	4.0 (at 298 K)	
H_2-V-Glycolate	163	1.3110	1.70 (at 77 K)	22 (at 77 K)	22
			0.35 (at 298 K)	4.9 (at 298 K)	
V-Glycolamide150	15	1.2390	1.40 (at 77 K)	17 (at 77 K)	27
			0.37 (at 298 K)	4.6 (at 298 K)	
AX-21	3225	2.103	4.2 (at 77 K, 65 bar)	14 (at 77 K, 65 bar)	13
			0.55 (at 298 K)		
MOF-5[(*)]	3534		5.1 (at 77 K)		5.5
			0.28 (at 298 K)		

[a] Data are taken at 85 bar. MOF adsorption data obtained from ref 41.

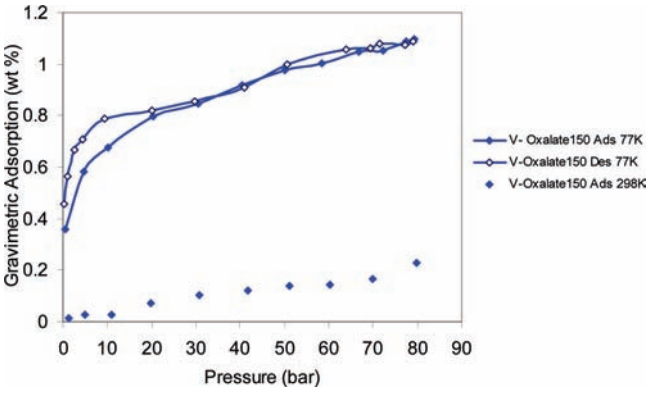

Figure 4. Hydrogen adsorption properties at 77 K, 298 K of V-Oxalate150. Desorption at 298 K is left out for clarity.

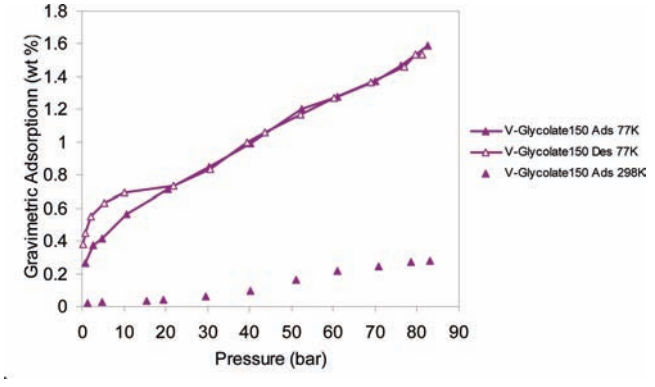

Figure 5. Hydrogen adsorption properties at 77 K, 298 K of V-Glycolate150. Desorption at 298 K is left out for clarity.

physisorption and is followed by a linear region increasing up to 1.1 wt % at 85 bar (Figure 2). A similar rise up to 0.5 wt % for

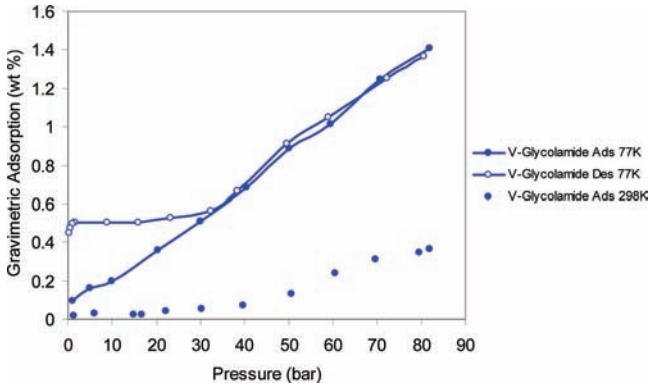

Figure 6. Hydrogen adsorption properties at 77 K, 298 K of V-Glycolamide150. Desorption at 298 K is left out for clarity.

V-Glycolate150, followed by linear adsorption up to 1.6 wt %, is also observed (Figure 3).

At room temperature and 85 bar, V-Oxalate150 and V-Glycolate150 adsorb 0.23 and 0.28 wt % of hydrogen, respectively. The V-Glycolamide150 material does not exhibit a sharp physisorption increase at low pressure and 77 K, and the adsorption isotherm is linear in the pressure range up to 85 bar, at which it absorbs 1.4 wt % hydrogen. A sharp increase is observed in the desorption, however, as it plateaus at 0 bar and 0.5 wt % hydrogen. Placing the sample under a vacuum after the desorption cycle removes this hysteresis as the second adsorption cycle is then identical to the first. The reason this behavior is not observed in V-Oxamide150 is not understood, but may be related to different pore structures in the material. This would introduce a slight kinetic barrier to initial adsorption and desorption at low pressure in this material, due to the low porosity and energy required for hydrogen diffusion through the void space within the materials.[42] Moreover, at 298 K and 85 bar, V-Glycolamide 150 adsorbs 0.37 wt % hydrogen, which is higher than that of H_2-V-Glycolate materials, even though the V-Glycolamide150 possesses

dx.doi.org/10.1021/ja110243r |J. Am. Chem. Soc. 2011, 133, 4955–4964

Table 2. V Concentration of Various Vanadium Materials and Average Number of Hydrogen Molecules Adsorbed on Each Vanadium Site at 85 bar[a]

material	number of H_2/V at 77 K	number of H_2/V at 298 K
V-Oxamide150	3.50	0.88
V-Oxalate150	1.19	0.25
H_2-V-Oxalate	1.42	0.45
V-Glycolate150	1.81	0.31
H_2-V-Glycolate	1.41	0.29
V-Glycolamide150	1.25	0.33

[a] Numbers calculated from experimental TGA results.

a much smaller nitrogen surface area. According to XPS results, V-Glycolamide150 possesses the second highest concentration of V(III) in the sample series, and these active species account for the hydrogen adsorption capacity, physisorption in this case representing minor adsorption capacity contribution.

Hysteretic adsorption−desorption was also observed in V-Oxalate150 and V-Glycolate150, however, to a much lower degree. At room temperature, V-Glycolamide150 adsorbs up to 0.37 wt % at 85 bar, which is higher than that of V-Oxalate150 and V-Glycolate150, but lower than observed in the V-Oxamide series. By comparing the gravimetric adsorption capacities at 298 and 77 K, the retention of excess adsorption capacities is calculated and ranges from 17% to 32%. These values are higher than those of MOF-5, which retains 5.5%,[37] and carbon AX-21, which retains 13%.[21]

To summarize these results, V-oxamide150 possesses both the lowest surface area and the highest excess storage capacities. The combination of low surface area and a high concentration of Kubas binding sites in this material minimizes physisorption, allowing the majority of adsorption to arise via the Kubas interaction. This is clearly seen in Table 2, which shows the comparison of H_2/V in the materials studied. On the basis of the TGA results, the oxamide material absorbs 3.5 H_2/V at 77 K and 0.88 H_2/V at 298 K, while the other materials range from 0.25 to 0.45 H_2/V (Table 2). By comparison, the vanadium hydrazides range in 1.13−1.96 H_2/V center;[22] the value of 3.5 H_2/V at 77 K reflects the presence of a component of physisorption in the total amount absorbed, introducing a systematic error in the H_2/V values. This accounts for the fact that the maximum allowable by the 18 electron rule with THF coordination is 2 H_2/V. Thus, a value of 2 H_2/V is more reasonable and compares to a value of 2.18 H_2/V at 77 K for a compressed pellet of this material (Figure S8). So, while not entirely accurate, these values are still useful benchmarks in comparing the relative efficiency of H_2 adsorption in these materials. Thus, while these materials possess lower gravimetric and volumetric capacities of the best vanadium hydrazide materials,[22] which exhibit 1.17 wt % and 23.2 kg H_2/m^3, the more controlled coordination environment around the V centers afforded by the oxamide ligand as compared to hydrazine, which can bond and bridge in several ways, may make these materials easier to study and characterize.

Using a variant of Clausius−Clapeyron I equation, the hydrogen adsorption enthalpies were calculated by employing two sets of adsorption data at 77 and 87 K. V-Oxamide100 and V-Oxamide150 possess adsorption enthalpies that rise versus surface coverage and from 2.3 to 19.8 kJ/mol H_2, approaching the 20−30 kJ/mol H_2 range, believed to be the ideal hydrogen

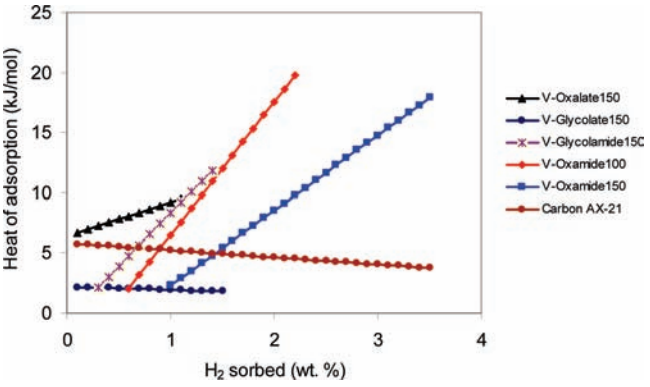

Figure 7. Hydrogen binding enthalpies of V-Oxamide100, V-Oxamide150, V-Oxalate150, V-Glycolate150, V-Glycolamide150, and carbon AX-21.

adsorption enthalpy (Figure 7).[13] This rising enthalpy trend has been observed in all materials studied in our group involving reduced early transition metal species, where the Kubas interaction is believed to be operative as an adsorption mechanism.[15] This phenomenon been predicted in calculations on Sc-coated buckyballs,[14] and evidence for the Kubas interaction in these and related materials was provided by recent ESR work on V-hydrazide gels.[22] V-Oxalate150 and V-Glycolamide150 exhibit adsorption heat in the range of 6.6−9.5 kJ/mol H_2 and 2.1−11.9 kJ/mol H_2, respectively. The lower enthalpies correspond with the lower hydrogen adsorption of these samples at 77 and 298 K. V-Glycolate150 possesses the lowest adsorption enthalpy at ~2 kJ/mol with traditional physisorption behavior that decreases with hydrogen concentration. This indicates that there is little or no Kubas binding in the mechanism of adsorption of this material.

A 20-cycle adsorption run with pressure up to 85 bar was carried out on the V-Oxamide150 sample. The result shows no significant loss of excess adsorption capacity through cycling (Figure S9, Supporting Information). The adsorption results range randomly between 0.82 and 0.91 wt %, falling within the instrument error (±0.05%, instrument's user manual), and the average adsorption capacity of this 20-cycle run is 0.87 wt %.

Hydrogenation was carried out on V-Oxalate150 and V-Glycolate150 according to Scheme 2 to replace residual mesityl groups with hydride ligands, using experimental conditions developed previously by our group.[19] Theoretical studies on the interaction of hydrogen with different ligands showed that transition metal species with hydride ligands possess higher heat of adsorption than those with alkyl, allyl, aryl, or benzyl groups.[20] This is because alkyl, allyl, aryl, or benzyl groups are stronger π-acceptors and exhibit more steric hindrance than hydride. Moreover, the removal of carbon will lead to a decrease in the sample weight and a concomitant increase in gravimetric hydrogen storage capacity. Thus, hydrogenation at 85 bar and 150 °C of V-Oxalate150 and V-Glycolate150 decreases the carbon concentration from 28.14% to 23.99% for V-Glycolate, while V-oxalate150 showed very little change. There was also an increase in vanadium concentration from 19.64 to 21.60 wt % in the V-Glycolate150 material, while again the V-Oxalate150 sample showed little change. The TGA results (Figure S7) showed 44.87% remaining mass after combustion for the hydrogenated V-Oxalate material as compared to 42.01% in the parent material, indicating that only a small amount of hydrocarbon had been removed. Likewise, 54.83% mass remained for the hydrogenated

dx.doi.org/10.1021/ja110243r | J. Am. Chem. Soc. 2011, 133, 4955–4964

Scheme 2. Proposed Hydrogenolysis Reactions of (a) V-Oxalate150 and (b) V-Glycolate150

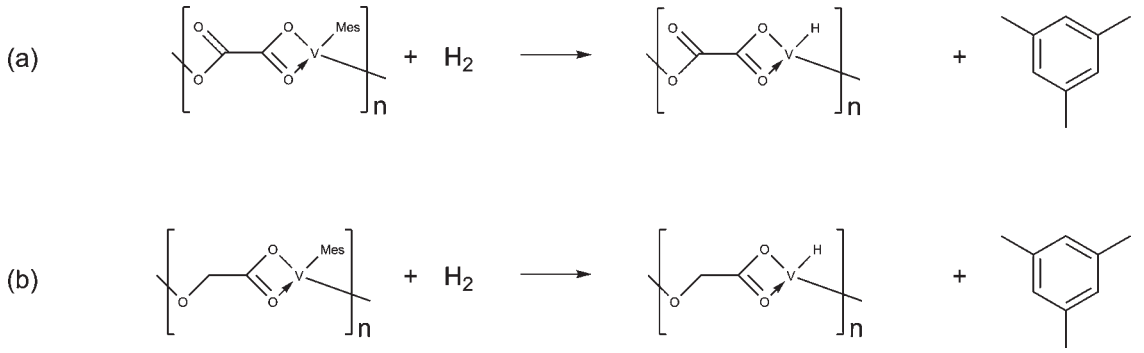

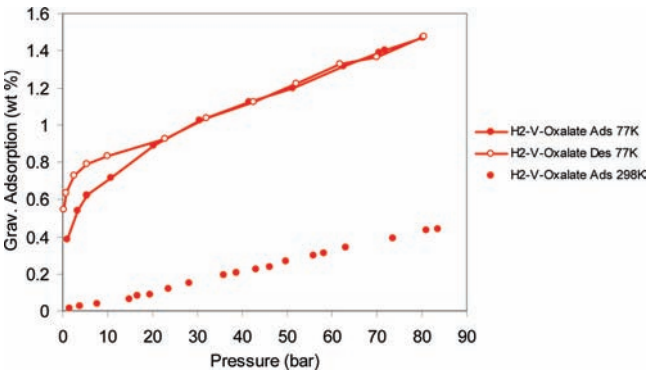

Figure 8. Hydrogen adsorption properties at 77 K, 298 K of H_2-V-Oxalate. Desorption at 298 K is left out for clarity.

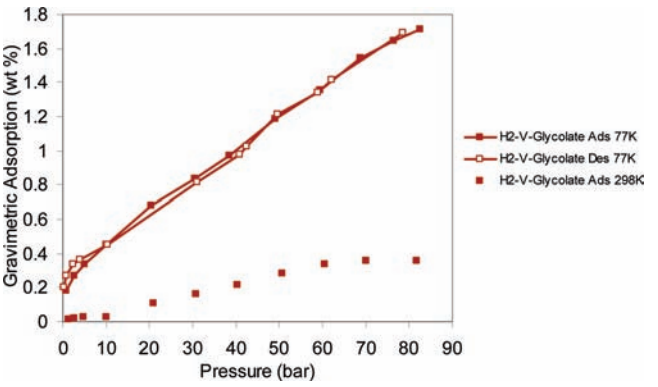

Figure 9. Hydrogen adsorption properties at 77 K, 298 K of H_2-V-Glycolate. Desorption at 298 K is left out for clarity.

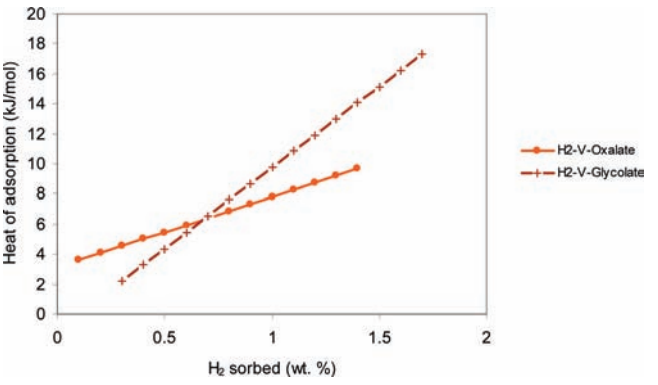

Figure 10. Hydrogen binding enthalpies of H_2-V-Oxalate150, H_2-V-Glycolate150.

V-Glycolate as compared to 49.13% in the starting material. If complete hydrogenation had occurred, TGA would show 65.39% and 72.18% mass remaining for the V-Oxalate and V-Glycolate materials, respectively. Hydrogenation of V-Glycolate150 led to a detectable decrease in surface area (from 220 to 163 m^2/g), but no significant change was observed in the surface area of the hydrogenated V-Oxalate150 material. The IR spectra of these materials both show a very minor decrease in the C−H stretch, indicating that only a small change has occurred in both samples. There was also little detectable change in the XPS spectra of either material. The difficulty in hydrogenating off the mesityl group from V was observed previously in silica supported vanadium mesityl fragments.[19]

Hydrogenation has a more pronounced effect in the hydrogen adsorption performance of V-Glycolate150 than that of V-Oxalate150 on the basis of elemental analysis and thermogravimetric analysis. H_2-V-Oxalate and H_2-V-Glycolate possess linear hydrogen adsorption isotherms from 0 to 85 bar at room temperature with better linearity than those of V-Oxalate150 and V-Glycolate150. The excess storage isotherms of H_2-V-Oxalate and H_2-V-Glycolate are shown in Figures 8 and 9, respectively. H_2-V-Oxalate demonstrated a rise to 0.7 wt % at 77 K and low pressure, after which the isotherm became linear and rose to 1.4 wt % at 85 bar, which is 0.3 wt % higher than the adsorption capacity of the non-hydrogenated V-Oxalate material. A 0.1 wt % adsorption increment with respect to the non-hydrogenated sample was observed at 77 K and 85 bar in H_2-V-Glycolate. The two hydrogenated materials possess linear adsorption isotherms at room temperature, H_2-V-Oxalate and H_2-V-Glycolate adsorbing up to 0.44 and 0.35 wt %, respectively. Increasing the hydrogenation reaction temperatures led to further decrease of carbon content for the V-Glycolate150 sample, but no enhancement of hydrogen adsorption capacities.

Heats of hydrogen adsorption of these two samples are calculated using adsorption isotherms at 77 and 87 K and are shown in Figure 10. In line with the negligible change in H_2-V-Oxalate on hydrogenation, there was little change in the enthalpy behavior or magnitude in this sample. In the case of H_2-V-Glycolate, however, hydrogenation leads to a dramatic increase in enthalpy, now rising from 2.2 to 17.3 kJ/mol H instead

dx.doi.org/10.1021/ja110243r |J. Am. Chem. Soc. 2011, 133, 4955–4964

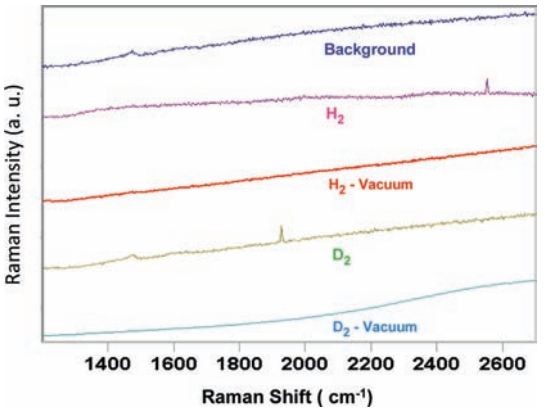

Figure 11. Raman spectra of V-Oxamide150 under H_2 and D_2.

of falling from 2.0 kJ/mol. The change in enthalpy behavior corresponds to a noticeable change in hydrogen adsorption capacity at 77 K and 85 bar (1.6−1.8 wt %) and the change in this material's composition. The enhancement of adsorption performance of H_2-V-Glycolate at 298 K and 85 bar (0.28−0.35 wt %) is smaller but still noticeable. The most likely reason for the increase in enthalpy and absorption is the opening of new more active V centers on loss of hydrocarbon ligand as evidenced by the EA results. However, this adsorption performance is much less than that of V-Oxamide150 because there are a limited number of Kubas hydrogen coordination sites available in V-Glycolate150 to begin with, so opening a small amount of sites of higher enthalpy only leads to a moderate change in gravimetric adsorption.

Vibrational spectroscopy studies were carried out to clarify the interaction between hydrogen and the adsorption centers. In previous work on vanadium hydrazides, we used ESR to confirm that V(III) was interacting with H_2 at room temperature.[22] Vibrational spectroscopy is a more traditional method of studying Kubas binding to metals because it potentially provides more direct information on the mode of hydrogen interaction with the metal, and the length of the H−H bond can be used to gauge the strength of the binding interaction.[43] A free H−H stretch is Raman active, but IR inactive, while coordinated M(H−H), which becomes formally IR allowed due to polarization along the M(H−H) axis, is weak or invisible unless coupled to other bands such as M(CO), and typically appears in the region from 2100 to 2700 cm^{-1}.[43] This band loses intensity and shifts to 1700−1900 cm^{-1} in the case of the D_2 analogue, demonstrating a smaller net isotope effect than observed for M−H(D).[43] In accordance with these expectations, V-Oxamide 150 shows no change in the IR on treatment with H_2 or D_2 at 1 bar for 1 h before sample preparation. After treatment with D_2 for several days, however, V-Oxamide150 exhibits a weaker intensity of the V−H band at 2200 cm^{-1} (Figure S9; Supporting Information), suggesting that a small amount of deuterium substitution has occurred.[29] This phenomenon could be attributed to the formation of a metastable VH(D_2) complex, which could yield either V−D or the original V−H after the sample is evacuated.

Figure 11 shows the Raman spectrum of V-Oxamide150 under H_2 followed by the same sample after evacuation, this evacuated sample under D_2, and finally this D_2 sample after vacuum. The sample prior to any treatment with H_2 or D_2 is also shown for reference. The strong band at 2553 cm^{-1} disappears under vacuum, and after treatment with D_2 a new band appears at 1927 cm^{-1}, which also disappears after vacuum. These results are consistent with Raman studies on previous Kubas compounds[43] and demonstrate for the first time that the rising enthalpies are indeed related to the Kubas interaction, as the ESR evidence in a previous report on V-hydrazides shows only that H_2 is interacting with the V(III) center, but does not give any information on the intimate nature of this interaction. The position and lower intensity of the υ(D−D) is expected on the basis of previous studies in the literature.[43] This is thus the first Raman evidence of the Kubas interaction in an extended solid in which the metals are a part of the framework structure. Previous work on MOFs with open metal sites suggested Kubas interactions but only Coulombic interactions were observed;[44−46] however, all Raman spectra showed little or no bathochromic shift expected for this bonding mode, all of the υ(H−H) appearing above 4000 cm^{-1}.[44] Raman spectroscopy has been performed on Cu-exchanged ZSM-5[16] and has shown a υ(H−H) of 3079 and 3130 cm^{-1}, indicative of a weak Kubas interaction; however, the Cu is not a part of the framework in this material, and υ(H−H) values are relatively high as compared to the majority of Kubas compounds in the literature.[43] Furthermore, in the design of materials exploiting the Kubas interaction for hydrogen storage, it is important that the metal comprises as large a fraction as possible of the overall weight of the system and is not just an ion or metal complex exchanged onto the surface of a much heavier structure that does not absorb H_2 in a Kubas fashion.

CONCLUSIONS

In summary, a series of new polymeric solids were synthesized by the reaction between $V(Mes)_3 \cdot THF$ with various polyprotic multidentate ligands. These polymers were designed with the aim of creating well-defined Kubas sites for hydrogen storage that could be studied by spectroscopy and gas sorption techniques. The V-Oxamide150 sample showed the highest performance with adsorption value of 3.49 wt % with adsorption enthalpy of 17.9 kJ/mol H_2 at 77 K. At 298 K, the materials adsorb 0.87 wt % at 85 bar with linear isotherms without reaching saturation, which increases the value of these materials at higher pressure. While these values fall short of the DOE goals, they are comparable to the best MOFs at 298 K and 80 bar. Raman spectroscopy and deuterium labeling confirmed the presence of Kubas binding in these solids, for the first time unequivocally tying the rising enthalpy trends observed previously in our systems based on low-valent metals to the Kubas interaction. The DOE guidelines specify a maximum pressure of 100 bar; however, commercial pressure vessels for hydrogen transport are normally rated at 200 bar or higher, and our materials possess linear isotherms that do not saturate at 298 K and 80 bar. We thus anticipate further gains not only on applying this strategy to different metal systems, but also recording isotherms at higher pressures.

ASSOCIATED CONTENT

Supporting Information. XRD, BET surface areas, IR spectroscopy, and XPS of all samples dried at 150 °C, elemental analysis, TGA, and adsorption of V-Oxamide150 compressed pellet, and the 20-cycle hydrogen adsorption run of V-Oxamide150. This material is available free of charge via the Internet at http://pubs.acs.org.

AUTHOR INFORMATION

Corresponding Author
dantonel@glam.ac.uk

■ ACKNOWLEDGMENT

NSERC is acknowledged for funding.

■ REFERENCES

(1) (a) Schlapbach, L.; Zuettel, A. *Nature* **2001**, *414*, 353. (b) Seayad, A. M.; Antonelli, D. M. *Adv. Mater.* **2004**, *16*, 765. (c) Yaghi, O. M.; O'Keeffe, M.; Ockwig, N. W.; Chae, H. K.; Eddaoudi, M.; Kim, J. *Nature* **2003**, *423*, 705. (d) Mark Thomas, K. *Dalton Trans.* **2009**, 1487. (e) Wang, L.; Yang, R. T. *Energy Environ. Sci.* **2008**, *1*, 268. (f) Lochan, R. C.; Head-Gordon, M. *Phys. Chem. Chem. Phys.* **2006**, *8*, 1357. (g) Eberle, U.; Felderhoff, M.; Schueth, F. *Angew. Chem., Int. Ed.* **2009**, *48*, 2. (h) Satyapal, S.; Petrovic, J.; Read, C.; Thomas, G.; Ordaz, G. *Catal. Today* **2007**, *120*, 246. (i) Liu, C.; Li, F.; Ma, L.-P.; Cheng, H.-M. *Adv. Mater.* **2010**, *22*, E28.

(2) (a) Langmi, H. W.; Book, D.; Walton, A.; Johnson, S. R.; Al-Mamouri, M. M.; Speight, J. D.; Edwards, P. P.; Harris, I. R.; Anderson, P. A. *J. Alloys Compd.* **2005**, *404*−*406*, 637. (b) Hirscher, M.; Panella, B. *Scr. Mater.* **2007**, *56*, 809. (c) Bénard, P.; Chahine, R. *Scr. Mater.* **2007**, *56*, 803. (d) Hu, Y. H.; Zhang, L. *Adv. Mater.* **2010**, *22*, E1. (e) Zhao, J.; Shi, J.; Zhang, X.; Cheng, F.; Liang, J.; Tao, Z.; Chen, J. *Adv. Mater.* **2010**, *22*, 394.

(3) (a) Orimo, S.; Nakamori, Y.; Eliseo, J. R.; Zuettel, A.; Jensen, C. M. *Chem. Rev.* **2007**, *107*, 4111. (b) Sandrock, G. *J. Alloys Compd.* **1999**, *293*, 877. (c) Bogdanovic, B.; Eberle, U.; Felderhoff, M.; Schueth, F. *Scr. Mater.* **2007**, *56*, 809.

(4) Hydrogen, Fuel Cells and Infrastructure Technologies Program: Multi-year Research, Development and Demonstration Plan: Planned Program Activities for 2005−2015. http://www1.eere.energy.gov/hydrogenandfuelcells/mypp/pdfs/storage.pdf; retrieved September 16th, 2009.

(5) Dornheim, M.; Doppiu, S.; Barkhordarian, G.; Boesenberg, U.; Klassen, T.; Gutfleisch, O.; Bormann, R. *Scr. Mater.* **2007**, *56*, 841.

(6) Graetz, J.; Reilly, J. J. *Scr. Mater.* **2007**, *56*, 835.

(7) Yang, R. T.; Wang, Y. *J. Am. Chem. Soc.* **2009**, *131*, 4224.

(8) (a) Strobel, R.; Garche, J.; Moseley, P. T.; Jorissen, L.; Wolf, G. *J. Power Sources* **2006**, *159*, 781.

(9) (a) Wong-Foy, A. G.; Matzger, A. J.; Yaghi, O. M. *J. Am. Chem. Soc.* **2006**, *128*, 3494. (b) Dailly, A.; Vajo, J. J.; Ahn, C. C. *J. Phys. Chem. B* **2006**, *110*, 1099. (c) Kaye, S. S.; Long, J. R. *J. Am. Chem. Soc.* **2005**, *127*, 6506. (d) Rosi, N. L.; Eckert, J.; Eddaoudi, M.; Vodak, D. T.; Kim, J.; O'Keeffe, M.; Yaghi, O. M. *Science* **2003**, *300*, 1127.

(10) Yan, Y.; Lin, X.; Yang, S.; Blake, A. J.; Dailly, A.; Champness, N. R.; Hubberstey, P.; Schroeder, M. *Chem. Commun.* **2009**, 1025.

(11) (a) Zhou, W.; Yildirim, T. *J. Phys. Chem. C* **2008**, *112*, 8132. (b) Dincă, M.; Dailly, A.; Liu, Y.; Brown, C. M.; Neumann, D. A.; Long, J. R. *J. Am. Chem. Soc.* **2006**, *128*, 12876.

(12) (a) Kubas, G. J.; Ryan, R. R.; Swanson, B. I.; Vergamini, P. J.; Wasserman, H. J. *J. Am. Chem. Soc.* **1984**, *106*, 451. (b) Kubas, G. J. *Chem. Rev.* **2007**, *107*, 4152. (c) Heinekey, D. M.; Lledós, A.; Lluch, J. M. *Chem. Soc. Rev.* **2004**, *33*, 175.

(13) (a) Vitillo, J. G.; Regli, L.; Chavan, S.; Ricchiardi, G.; Spoto, G.; Dietzel, P. D. C.; Bordiga, S.; Zecchina, A. *J. Am. Chem. Soc.* **2008**, *130*, 8386. (b) Dincă, M.; Long, J. R. *Angew. Chem., Int. Ed.* **2008**, *47*, 6766.

(14) Zhao, Y.; Kim, Y.; Dillon, A. C.; Heben, M. J.; Zhang, S. B. *Phys. Rev. Lett.* **2005**, *94*, 155504.

(15) Hoang, T. K. A.; Antonelli, D. M. *Adv. Mater.* **2009**, *21*, 1787.

(16) Georgiev, P. A.; Albinati, A.; Mojet, B. L.; Ollivier, J.; Eckert, J. *J. Am. Chem. Soc.* **2007**, *129*, 8086.

(17) Hamaed, A.; Trudeau, M.; Antonelli, D. M. *J. Am. Chem. Soc.* **2008**, *130*, 6992.

(18) (a) Hoang, T. K. A.; Hamaed, A.; Trudeau, M.; Antonelli, D. M. *J. Phys. Chem. C* **2009**, *113*, 17240. (b) Hu, X.; Trudeau, M.; Antonelli, D. M. *Chem. Mater.* **2007**, *19*, 1388. (c) Hamaed, A.; Hoang, T. K. A.; Trudeau, M.; Antonelli, D. M. *J. Organomet. Chem.* **2009**, *694*, 2793.

(19) Hamaed, A.; Mai, H. V.; Hoang, T. K. A.; Trudeau, M.; Antonelli, D. M. *J. Phys. Chem. C* **2010**, *114*, 8651.

(20) Skipper, C.; Hamaed, A.; Antonelli, D.; Kaltsoyannis, N. *J. Am. Chem. Soc.* **2010**, *132*, 17296.

(21) Mai, H. V.; Hoang, T. K. A.; Hamaed, A.; Trudeau, M.; Antonelli, D. M. *Chem. Commun.* **2010**, *46*, 3206.

(22) Hoang, T. K. A.; Webb, I. M.; Mai, H. V.; Hamaed, A.; Walsby, C. J.; Trudeau, M.; Antonelli, D. M. *J. Am. Chem. Soc.* **2010**, *132*, 11792.

(23) Langmi, H. W.; Walton, A.; Ah-Mamouri, M. M.; Johnson, S. R.; Book, D.; Speight, J. D.; Edwards, P. P.; Gameson, I.; Anderson, P. A.; Harris, I. R. *J. Alloys Compd.* **2003**, *356*−*357*, 710.

(24) Seidel, V. W.; Kreisel, G. *Z. Anorg. Allg. Chem.* **1977**, *435*, 146.

(25) Hu, X.; Skadtchenko, B. O.; Trudeau, M.; Antonelli, D. M. *J. Am. Chem. Soc.* **2006**, *128*, 11740.

(26) Furukawa, H.; Miller, M. A.; Yaghi, O. *J. Mater. Chem.* **2007**, *17*, 3197.

(27) Seidel, W.; Kreisel, G. *Z. Chem.* **1974**, *14*, 25.

(28) Gregg, S. J.; Sing, K. S. W. *Adsorption, Surface Area and Porosity*, 2nd ed.; Academic Press: London, 1982; pp 41−42.

(29) Heinekey, D. M.; Oldham, W. J., Jr. *Chem. Rev.* **1993**, *93*, 913.

(30) Antonelli, D. M.; Schaefer, W. P.; Parkin, G.; Bercaw, J. E. *J. Organomet. Chem.* **1993**, *462*, 213.

(31) Groenenboom, C. J.; Sawatzky, G.; Meijer, H. J. D.; Jellinek, F. *J. Organomet. Chem.* **1974**, *76*, C4–C6.

(32) Horvath, B.; Strutz, J.; Geyer-Lippmann, J.; Horvath, E. G. *Z. Anorg. Allg. Chem.* **1981**, *483*, 181.

(33) Kasperkiewicz, J.; Kovacich, J. A.; Lichtman, D. *J. Electron Spectrosc. Relat. Phenom.* **1983**, *32*, 123.

(34) Wagner, C. D.; Riggs, W. M.; Davis, L. E.; Moulder, J. F.; Muilenberg, G. E. *Handbook of X-Ray Photoelectron Spectroscopy: Physical Electronics Division*; Perkin-Elmer Corp.: Eden Prairie, MN, 1979.

(35) Whelan, C. M.; Cecchet, F.; Baxter, R.; Zerbetto, F.; Clarkson, G. J.; Leigh, D. A.; Rudolf, P. *J. Phys. Chem. B* **2002**, *106*, 8739.

(36) Sivastava, S.; Badrinarayanan, S.; Mukhedkar, A. J. *Polyhedron* **1985**, *4*, 409.

(37) Batich, C. D.; Donald, D. S. *J. Am. Chem. Soc.* **1984**, *106*, 2758.

(38) Gervais, M.; Douy, A.; Gallot, B.; Erre, R. *J. Colloid Interface Sci.* **1988**, *125*, 146.

(39) Larkins, F. P.; Lubenfeld, A. *J. Electron Spectrosc. Relat. Phenom.* **1979**, *15*, 137.

(40) Kafizas, A.; Hyett, G.; Parkin, I. P. *J. Mater. Chem.* **2009**, *19* 1399.

(41) Panella, B.; Hirscher, M.; Puetter, H.; Mueller, U. *Adv. Funct. Mater.* **2006**, *16*, 520.

(42) (a) Kang, J.; Wei, S.-H.; Kim, Y.-H. *J. Am. Chem. Soc.* **2010**, *132*, 1510. (b) Yamada, K.; Tanaka, H.; Yagashita, S.; Adachi, K.; Uemura, T.; Kitagawa, S.; Kawata, S. *Inorg. Chem.* **2006**, *45*, 4322.

(43) Bender, B. R.; Kubas, G. J.; Jones, L. H.; Swanson, B. I.; Eckert, J.; Capps, K. B.; Hoff, C. D. *J. Am. Chem. Soc.* **1997**, *119*, 9179.

(44) Murray, L. J.; Dincă, M.; Long, J. R. *Chem. Soc. Rev.* **2009**, *38*, 1294.

(45) Kaye, S. S.; Long, J. R. *J. Am. Chem. Soc.* **2008**, *130*, 806.

(46) Centrone, A.; Siberio-Pérez, D. Y.; Millward, A. R.; Yaghi, O. M.; Matzger, A. J.; Zerbi, G. *Chem. Phys. Lett.* **2005**, *411*, 516.